This article has been accepted for publication in Journal of Neurology, Neurosurgery & Psychiatry, 2020 following peer review, and the Version of Record can be accessed online at https://doi.org/10.1136/jnnp-2019-322242

Cognitive inhibition impairments in presymptomatic *C9orf72* carriers

Maxime Montembeault[1,2], Sabrina Sayah[1], Daisy Rinaldi[1,3], Benjamin Le Toullec[1,3], Anne Bertrand[1,4,5], Aurélie Funkiewiez[3,6], Dario Saracino[1,3], Agnès Camuzat[1], Philippe Couratier[7,8], Marianne Chouly[7,8], Didier Hannequin[9,10], Carole Aubier Girard[9,10], Florence Pasquier[11], Xavier Delbeuck[11], Olivier Colliot[1,4,12], Bénédicte Batrancourt[1], Carole Azuar[3,6], Richard Lévy[1,3,6], Bruno Dubois[1,3,6], Isabelle Le Ber*[1,3,6], Raffaella Migliaccio*[1,3,6], PrevDemAls study group

[1] Sorbonne Universités, Université Pierre et Marie Curie Paris 06, Institut National de la Santé et de la Recherche Médicale, Centre National de la Recherche Scientifique, Institut du Cerveau et la Moelle Épinière, FrontLAB, Hôpital Pitié-Salpêtrière, Assistance Publique–Hôpitaux de Paris, Paris, France
[2] Memory & Aging Center, University of California in San Francisco, San Francisco, United-States
[3] Reference Centre for Rare of Early Onset Dementias, Hôpital Pitié-Salpêtrière, Assistance Publique–Hôpitaux de Paris, Paris, France
[4] Aramis Project Team, Inria Research Center of Paris, Paris, France
[5] Department of Neuroradiology, Hôpital Pitié-Salpêtrière, Assistance Publique–Hôpitaux de Paris, Paris, France
[6] Institute of Memory and Alzheimer's Disease, Centre of Excellence of Neurodegenerative Disease, Department of Neurology, Hôpital Pitié-Salpêtrière, Assistance Publique–Hôpitaux de Paris, Paris, France
[7] Centre de Référence SLA et autres maladies du motoneurone, Centre Hospitalier Universitaire de Limoges, Limoges, France
[8] Centre de Compétence Démences Rares, Centre Hospitalier Universitaire de Limoges, Limoges, France
[9] Centre National de Référence pour les Malades Alzheimer Jeunes, Centre Hospitalier Universitaire de Rouen, INSERM 1245, Rouen, France
[10] Department of Neurology, Centre Hospitalier Universitaire de Rouen, Rouen, France
[11] Université de Lille, INSERM U1171, Centre de la mémoire (CMRR), Centre national de référence pour les malades Alzheimer jeunes (CNRMAJ), CHU Lille, Development of Innovative Strategies for a Transdisciplinary approach to ALZheimer's disease (DistAlz), Lille, France
[12] Centre pour l'Acquisition et le Traitement des Images, Institut du Cerveau et la Moelle Épinière, Paris, France

*These authors contributed equally.

Correspondence to:
Dr. Raffaella Migliaccio, ICM, 47 bd de l'hopital, 75013 Paris, France. Telephone number: 0033 1 57 27 41 43; E-mail address: lara.migliaccio@gmail.com and lara.migliaccio@icm-institute.org

Word count: 3513
Number of references: 50

ABSTRACT

Objective: To investigate cognitive inhibition in pre-symptomatic *C9orf72* mutation carriers (C9+) and its associated neuroanatomical correlates.

Methods: Thirty-eight pre-symptomatic *C9orf72* mutation carriers (C9+, mean age 38.2±8.0 years old) and 22 C9- controls from the PREV-DEMALS cohort were included in this study. They underwent a cognitive inhibition assessment with the Hayling Sentence Completion Test (HSCT; Time to completion (part B - part A); error score in part B) as well as a 3D MRI.

Results: C9+ individuals younger than 40 years had higher error scores (part B) but equivalent HSCT time to completion (part B - part A), compared to C9- individuals. C9+ individuals older than 40 years had both higher error scores and longer time to completion. HSCT time to completion significantly predicted the proximity to estimated clinical conversion from pre-symptomatic to symptomatic phase in C9+ individuals (based on the average age at onset of affected relatives in the family). Anatomically, we found that HSCT time to completion was associated with the integrity of the cerebellum.

Conclusion: The HSCT represents a good marker of cognitive inhibition impairments in C9+ and of proximity to clinical conversion. This study also highlights the key role of the cerebellum in cognitive inhibition.

Key-words: C9orf72 mutation; cognitive inhibition; Hayling Sentence Completion Test; voxel-based morphometry; cerebellum.

INTRODUCTION

Cognitive inhibition refers to the ability to resist to interference from irrelevant stimuli and is critical to manage everyday tasks. The Hayling Sentence Completion Test (HSCT) has been highlighted as an ecological cognitive inhibition task due to its ability to predict everyday functioning [1] and its resemblance to real-life inhibitory demands, such as the ability to suppress inappropriate words forms is part of many social interactions [2]. Clinically, the HSCT has been used in many populations presenting with disinhibition, such as patients with Alzheimer's disease, Parkinson's disease, progressive supranuclear palsy, bipolar disorder and finally, patients with cerebrovascular accidents or tumors [3-7]. Neuroimaging studies suggest that the HSCT is mainly associated with frontal damage [5-11]. In frontotemporal dementia (FTD) patients, the HSCT has also shown to be highly sensitive to cognitive inhibition impairments [8-12].

The HSCT therefore represents an interest for pre-symptomatic carriers of chromosome 9 open reading frame 72 (*C9orf72*) mutation, which is the most frequent genetic cause of FTD and amyotrophic lateral sclerosis (ALS) [13 14]. Little is known on cognitive inhibition abilities of pre-symptomatic individuals carrying *C9orf72* expansion (C9+), and very few studies have investigated cognition in general at this very early stage of FTD. While some authors did not detect any cognitive change in these individuals [15-17], others have identified specific cognitive changes in executive, praxis or memory even many years before the expected disease onset (for a review, see Table 1) [18-21]. All together, these studies have provided inconsistent results across cognitive functions, and no study has identified a direct relationship between cognitive and neuroanatomical changes.

Many neuroimaging studies have demonstrated that even if still in the pre-symptomatic phase, C9+ individuals already present with brain damage in frontal, temporal, parietal lobes as well as the thalami, the caudate nuclei, the cerebellum, the striatum and several white matter fascicles [15-23]. In particular, subtle cognitive, structural, and microstructural alterations can be detected very early in *C9orf72* carriers younger than 40 years [18]. However, despite the growing interest in these populations of individuals likely to be treated before developing the disease, there are still no relevant clinical and cognitive tools to detect early signs of impairments or able to predict the proximity to clinical conversion.

Within this framework, our aims were 1) to study cognitive inhibition performances in a large group of C9+ individuals using the HSCT; 2) to explore HSCT performances splitting C9 individuals according to age (younger and older than 40 years old, the latter group supposed to be closer to the disease onset); 3) to determine the ability of the HSCT to predict proximity to estimated clinical conversion from pre-symptomatic to symptomatic phase in C9+ individuals (based on the average age at onset of affected relatives in the family); 4) to investigate the neuroanatomical correlates of cognitive inhibition as assessed by the HSCT.

We hypothesized that all C9+ individuals would be impaired on the HSCT compared to C9- healthy subjects (including individuals under the age of 40 years), that the HSCT could be a useful tool to predict estimated time to disease onset in C9+ individuals, and that frontal regions would be correlated with poor cognitive inhibition.

Table 1. Review of studies investigating cognitive changes in pre-symptomatic C9+ versus C9- individuals

Study	n	Mean age (SD)	Mean estimated time to disease onset (SD)	Mean age at family onset (SD)	Discriminant tests	Non-discriminant tests
Panman et al., 2019	12	49.7 (12.4)	-	-	-	▪ MMSE ▪ NPI
Bertrand et al., 2018	41	39.8 (11.1)	19.3 (11.2)	-	▪ "Batterie d'Évaluation des Praxies" ▪ Free and cued recall test	▪ MMSE ▪ MDRS ▪ FBI ▪ FAB ▪ Mini-SEA ▪ Benson figure ▪ BNT ▪ Semantic fluency ▪ Letter fluency
Popuri et al., 2018	15	42.6 (11.3)	13.7 (11.2)	-	-	▪ MMSE ▪ FAB ▪ FBI
Papma et al., 2017	18	45.8 (13.8)	-	53.0 (5.3)	▪ Letter fluency ▪ Stroop Test	▪ MMSE ▪ FAB ▪ NPI ▪ BDI ▪ CBI-R ▪ BNT ▪ Semantic Association Test ▪ Semantic fluency ▪ RAVLT ▪ Digit span ▪ Trail Making Test ▪ LDST ▪ Ekman faces ▪ Happé theory of mind ▪ Clock Drawing Test ▪ Block design

Lee et al., 2016	15	43.7 (10.2)	8.2 (11.0)	51.8 (5.3)	▪CVLT (short form)	▪MMSE ▪Benson Figure ▪VOSP ▪Calculations ▪BNT ▪Wide range achievement test 4 ▪Digit span ▪Modified trails ▪Stroop test ▪Letter fluency ▪Semantic fluency ▪Design fluency ▪NPI ▪CATS ▪IRI ▪GDS
Walhout et al., 2015	16	45.5 (14.7)	-	-	-	▪FAB ▪Edinburgh Cognitive and Behavioral ALS screen

Abbreviations: Beck Depression Inventory = BDI; Boston Naming Test = BNT; California Verbal Learning Test = CVLT; Cambridge Behavioural Inventory-Revised = CBI-R; Comprehensive affective testing system = CATS; Frontal Assessment Battery = FAB; Frontal Behavior Inventory = FBI; Geriatric depression scale = GDS; Interpersonal reactivity index = IRI; Letter Digit Substitution Test = LDST; Mattis Dementia Rating Scale = MDRS; Mini-Mental State Exam = MMSE; Mini Social cognition and Emotional Assessment = Mini-SEA; Neuropsychiatric inventory = NPI; Rey Auditory Verbal Learning Test = RAVLT; SD = Standard deviation; Visual object and space perception battery = VOSP.

METHODS

Participants

Subjects from the PREV-DEMALS national multicentric study with available HSCT and MRI data were included in the present study. Only the subjects investigated in one centre, Pitié-Salpêtrière hospital, were included. This study was approved by the Comité de Protection des Personnes Ile de France VI of the Hôpital Pitié-Salpetrière, and written informed consent was obtained from all participants. All the details of the study have been previously described [18].

Sixty first-degree relatives of *C9orf72* mutation carriers from 37 families were included. Thirty-Eight participants carried a pathogenic expansion (>23 GGGGCC repeats; C9+); 22 healthy controls did not carry this expansion (C9−). Expected ages at onset of C9+ were estimated by subtracting the age of the participant at assessment to the mean age at symptoms onset within the family, as performed in other studies[21]. Demographic and general cognitive characteristics are presented in Table 2.

Cognitive study

Hayling Sentence Completion Test (HSCT)

Cognitive inhibition was assessed using the francophone version of the HSCT, a test consisting of two parts in which participants are asked to complete a series of sentences [24 25]. In part A (initiation condition), participants must complete 15 sentences as quickly as possible using the contextually predicted word (e.g.: "The postman was bitten by a"; Response: Dog). In part B (inhibition condition), participants must complete 15 sentences as rapidly as possible using a completely unconnected word, which requires inhibiting an automatic response. Two outcome measures were calculated: 1) the total time in seconds taken to complete every sentence in part A subtracted from the total time taken to complete every sentence in part B (Time to completion (part B – part A)); 2) an error score for the part B computed using the scoring system suggested by Burgess & Shallice [24]. A 3-point error score was given for an item in which the participant completed the sentence using the predicted word. A 1-point error score was given for an item in which the participant completed the sentence using a semantically related word. A 0-point error score was given

for good responses. Thus, for both outcome measures, a higher score indicates a worse performance.

Statistical analyses

The first analysis aimed at comparing the performance of presymptomatic C9+ and C9- individuals on the HSCT, taking into account the dependence of observations from individuals in the same family (cluster effect) and controlling for age, sex and education. Group means were estimated using generalized estimated equations (GEE) with an exchangeable covariance structure and a multivariable linear regression analysis (distribution: normal; link function: identity). Performance on the HSCT was the dependent variable and group (C9+/C9-), age, sex and education were the predictors. The estimated group means were compared with a statistical threshold of $p \leq 0.05$. Two separate GEE models were computed: one using time to completion (part B – part A) as a measure of HSCT performance and one using the error scores (part B). This analysis was first conducted on the whole group, then separating individuals based on age (younger and older than 40 years) to determine the effect of age. We chose a cut-off of 40 years old based on the average of age in our population, and also to remain consistent with a previous study from our group[18].

The second analysis aimed at assessing the ability of the HSCT performance to predict proximity to estimated clinical conversion from pre-symptomatic to symptomatic phase in C9+ individuals (based on the average age at onset of affected relatives in the family), taking into account the dependence of observations from individuals in the same family (cluster effect) and controlling for sex and education. We performed generalized

estimated equations (GEE) using an exchangeable correlation structure, a normal distribution and an identity link function. Expected time to disease onset was the dependent variable and HSCT performance, sex and education were the predictors. Two separate GEE models were computed: one using time to completion (part B – part A) as a measure of HSCT performance and one using the error scores.

MRI study

Acquisition

All scans were acquired on a Siemens Prisma Syngo 3T. Parameters of the 3D T1 sequence were as follow: spatial resolution = (1.1x1.1x1.1) mm3; TE/TR = 2.8-3ms/minimum; Bandwidth: 240-255 Hz.

Voxel-based morphometry: pre-processing

Structural images were preprocessed using voxel-based morphometry (VBM) implemented in SPM12 using MATLAB 7.14.0.739 (Mathworks, Natick, MA). The images were segmented into grey (GM) and white matter. Affine registered tissue segments were used to create a custom template using the DARTEL (diffeomorphic anatomical registration using exponentiated lie algebra) approach [26]. For each participant, the flow fields were calculated during a template creation, which described the transformation from each native GM image to the template. These were then applied to each participant's GM image. The VBM analysis was based on modulated GM images, where the GM value for each voxel was multiplied by the Jacobian determinant derived from spatial normalization to preserve the total amount of GM from the original images [27]. The resulting modulated and normalized images were then smoothed with a Gaussian kernel of 8mm FWHM.

Statistical analyses

Whole-brain VBM analyses were performed on smoothed GM images. First, the HSCT time to completion (Part B - Part A) and error score were entered as covariates of interest in two separate multiple regression statistical models including all subjects, with age, sex and total intracranial volume as nuisance covariates. The correlation was tested using a [-1] t-contrast, assuming that higher scores (which indicate worse performances) would be associated with decreased GM volumes. The significance of each effect of interest was determined using the theory of Gaussian fields. A statistical threshold of $p \leq .05$ family-wise error rate corrected at cluster level was used.

RESULTS

Table 2. Demographic characteristics

	C9-	C9+	*p* value
n	22	38	-
Sex (F/M)	13/9	22/16	.928
Education (Secondary/Higher education)	5/17	8/30	.879
Age (mean±SD)	40.3 (11.2)	38.2 (8.0)	.406
Age (range)	21-61	24-56	-
Expected time to disease onset	-	21.1 (8.4)	-
MMSE	29.0 (1.2)	28.7 (1.4)	.336
FAB	17.0 (1.4)	17.3 (0.9)	.407

MMSE=Mini-Mental State Exam; FAB=Frontal Assessment Battery

Group comparison of performance on the HSCT

C9+ individuals presented a significantly slower mean HSCT time to completion (part B – part A) in comparison to C9- individuals ($p \leq .05$) (Table 3, Figure 1). C9+ individuals also presented a significantly higher HSCT error scores (part B) in comparison to C9- individuals ($p \leq .001$) (Table 3, Figure 1). Of note, C9- individuals obtained results on the HSCT that were largely comparably to those of the healthy controls previously

published (error score: 2.0 ±1.9 in the present study vs. 2.3 ± 4.2)[12]. To confirm that these results were not biased by outliers, we identified any data points that are more than 1.5 box-lengths (or interquartile range) from the edge of their group boxplot (Figure 1). For HSCT time to completion, there were 3 outliers in the C9- group. For HSCT error scores, there were 1 outlier in the C9+ group and 3 outliers in the C9- group. When these outliers were removed from the analyses, the results were still significant (i.e. significantly higher HSCT time to completion and error scores in C9+ individuals).

When restricting the same analyses to participants younger than 40 years old (C9+ n = 22, mean age = 32.7±5.2, mean expected time to onset = 24.9±7.9; C9- n = 12, mean age = 31.9±5.9), C9+ individuals presented equivalent time to completion (part B – part A) in comparison to C9- individuals (p = .297), but they had higher error scores (p = .034). In participants older than 40 years old (C9+ n = 16, mean age = 45.7±4.2, mean expected time to onset = 15.7±5.8; C9- n = 10, mean age = 50.3±6.8), both HSCT time to completion (p < .001) and error score (p < .001) were higher in C9+ in comparison to C9- individuals.

Table 3. Group comparisons of performance on the HSCT

Variable	**Raw mean (standard deviation)**		**Adjusted mean (standard error)***		**Adjusted means difference (standard error)**	***p* value**
	C9- (n=22)	**C9+ (n=38)**	**C9- (n=22)**	**C9+ (n=38)**		
HSCT– Time to completion (part B – part A)	32.6 (±21.4)	47.1 (±26.2)	33.3 (±5.0)	46.4 (±4.2)	13.1 (±5.7)	.021
HSCT– Error score (Part B)	2.0 (±1.9)	3.6 (± 2.7)	2.1 (±0.4)	4.3 (±1.8)	2.3 (±0.7)	.001

*Estimated means and standard errors based on GEE model taking into account cluster effect of children in family and controlling for age, sex and education.

Ability of the HSCT performance to predict expected time to disease onset in C9+ individuals

In C9+ individuals, HSCT completion time (part B – part A) significantly predicted expected time to disease onset ($\beta = .143$ ($\pm .05$); Wald chi-square = 7.88; df = 1; $p = .005$). Sex and education were not significant predictors. Overall, this suggests that higher HSCT completion time predict the proximity to disease onset in C9+ individuals, in agreement with our previous result on C9+ older than the age of 40 years. HSCT error score did not significantly predict expected time to disease onset ($\beta = .925$ ($\pm .48$); Wald chi-square = 3.78; df = 1; $p = .052$).

Neuroanatomical correlates of HSCT performance

HSCT time to completion (Part B - Part A) correlated with GM volume in a large cluster in the left cerebellum ($p \leq .05$ FWE cluster level corrected; cluster extent: 2132 voxels). Peak significance was observed in the left cerebellar lobule VI (-18, -57, -14; t value = 4.93). The cluster also included the left cerebellar lobules IV-V (-5; -45; -12; t value =3.94), the left vermis (-3, -66, -10; t value = 3.36) and the left cerebellar lobule crusI (-13, -68, -27; t value = 3.29).

The HSCT error score (Part B) did not correlate with GM volume in any voxel.

Post-hoc analysis: Cerebellar GM correlates of HSCT time to completion

The whole-brain VBM analysis identified the left cerebellum as a GM correlate of HSCT time to completion (part B – part A). However, traditional VBM analysis is not ideal to investigate the cerebellum, because it relies on the ICBM12 template which provides

very little contrast for cerebellar structures and normalization to this template leads to a large spatial spread of individual fissures [28-31]. We therefore ran a post-hoc analysis using a toolbox specifically designed to resolve these limitations, the Spatially Unbiased Infratentorial Toolbox (SUIT) [28-31]. The aims of the post-hoc analyses were to: 1) confirm the result obtained in our traditional VBM analysis (HSCT time to completion correlated with GM volume in the left cerebellum across our sample); 2) investigate GM correlates of HSCT in C9+ individuals specifically.

Preprocessing

Preprocessing was conducted using SUIT (v.3.4) implemented in SPM12 [28-31]. First, the infratentorial area was isolated from the images and segmented into GM and white matter to obtain a cerebellar mask (suit_isolate_seg function). A normalization of the cerebellar mask to the SUIT atlas space was then conducted (suit_normalize_dartel function). During this step, flow fields (which describe the transformation from each native GM image to the template) are also calculated for each participant. These were then applied to each participant's GM image to reslice them into the SUIT space (suit_reslice_dartel function with modulation).

Results

Similarly to the whole-brain VBM analysis, HSCT time to completion (Part B - Part A) correlated with GM volume in the left cerebellar lobule VI ($p \leq .05$ FWE cluster level corrected), as displayed in Figure 2a and Table 4. Three other clusters were also significant, namely the right cerebellar lobule VIIIb, the right cerebellar lobule IX and the right cerebellar lobule VI.

When restricting the analysis to C9+ individuals, the correlation between HSCT time to completion and the cerebellum remained significant, although the significant cluster was located in the vermis ($p \leq .05$ FWE cluster level corrected), as displayed in Figure 2b and Table 4. Peak significance was observed in the left vermis crusII and the cluster also included the right vermis VIIb.

Table 4. Cerebellar GM correlates of HSCT time to completion (part B – part A) obtained by using the Spatially Unbiased Infratentorial Toolbox (SUIT) toolbox.

	Region	x	y	z	T value	Cluster extent	Sig.
Complete sample	**R lobule VIIIb**	**14**	**-44**	**-56**	**4.50**	**555**	**.000**
	R lobule IX	13	-49	-52	3.99	s.c.	
	R lobule IX	**6**	**-54**	**-51**	**4.20**	**173**	**.040**
	R lobule VI	**38**	**-47**	**-26**	**4.18**	**350**	**.002**
	R lobule VI	35	-62	-26	3.59	s.c.	
	R lobule crusI	33	-63	-35	3.76	s.c.	
	R lobule crusI	35	-51	-34	3.28	s.c.	
	L lobule VI	**-21**	**-54**	**-26**	**4.11**	**240**	**.011**
	L lobule VI	-17	-57	-14	3.76	s.c.	
C9+ only	**L vermis crusII**	**-1**	**-72**	**-33**	**5.99**	**162**	**0.40**
	R vermis VIIb	3	-69	-31	4.16	s.c.	

s.c. = same cluster

DISCUSSION

The present study reports on the potential of the HSCT to characterize and detect cognitive inhibition deficits in pre-clinical settings. We demonstrated that the HSCT was able to discriminate between C9+ and C9- individuals many years before the supposed disease onset (mean expected time to disease onset of 21.1 years), more significantly in individuals over 40 years old who are supposed to be closer to the disease onset. Furthermore, in C9+ individuals, HSCT time to completion significantly predicted estimated time to disease onset. Surprisingly and in contrast with our initial hypothesis, the performance on this test were not associated with frontal areas but with the integrity of the cerebellum, a key region associated with the *C9orf72* mutation.

Our study is one of the first to identify a discriminant and early cognitive marker in C9+ individuals (Table 1). In previous studies, other neuropsychological tests involving cognitive inhibition functioning such as the Stroop Test provided inconsistent results [19 20]. The Trail Making Test, which also assesses cognitive flexibility, did not allow for the detection of significant differences between C9+ and C9- individuals [19 20]. Other candidates for early cognitive markers in pre-symptomatic C9+ individuals might include memory and praxis tests (Table 1), although their ability to predict estimated proximity to conversion to symptomatic phases and their neural correlates have not been clarified in this population. In pre-symptomatic MAPT and GRN mutation carriers, letter fluency, categorical fluency and ScreeLing phonology tasks were shown to predict clinical conversion [32]. This highlights the interest of the HSCT as an assessment tool in this population and suggests that cognitive inhibition might be amongst the first cognitive functions showing subtle changes in C9+ individuals. The HSCT was selected because previous studies suggest that it is potentially more ecologically valid than traditional

inhibition tests since it has more resemblance to real-life inhibitory demands, as the ability to suppress inappropriate words forms is part of many social interactions [2]. Nonetheless, whether the identified cognitive inhibition changes manifest as subtle real-life disinhibition behaviors in C9+ individuals remain to be assessed. Our results are in line with the symptomatic phases of the *C9orf72*, in which cognitive inhibition impairments play a key role and in which the HSCT is also one of the most discriminative tools[8 10]. Furthermore, we have shown that lower performance on the HSCT (slower HSCT time to completion) significantly predicts closer proximity to disease onset in C9+ individuals. The time of completion was also significantly impaired in C9+ individuals older than 40 years, who are supposed to be closer to the disease onset. These findings provide evidence for the HSCT as an easy marker of progression from pre-symptomatic to symptomatic phase. This test can be easily applied in future studies of potential disease-modifying treatments against FTD and ALS to select the population.

In addition to the utility of the HSCT in the clinical/cognitive assessment of C9+, we showed for the first time that performance on the HSCT is associated with gray matter volume in the cerebellum (i.e. lower cerebellar volumes are associated with lower performance). This result is of great significance because recently the cerebellum has been unveiled as playing a key role in the *C9orf72* mutation. First, from a pathology perspective, the cerebellum is a key locus of tissue pathology in C9+ patients as demonstrated in many *post-mortem* studies [33 34]. Moreover, many *in vivo* studies reported a significant cerebellar atrophy on both presymptomatic [20-22] and symptomatic *C9orf72* patients [35-39]. Functionally, the cerebellum also appears disconnected from different brain networks affected in C9+ individuals, such as the salience, default mode, sensorimotor, and medial pulvinar

thalamus-seeded networks [19]. Connectivity studies have shown that the cerebellum is extensively connected with the prefrontal cortex *via* the thalamus [40], which are both key regions in FTD. The thalamus, in particular, seems early involved in the pathological brain damage in *C9orf72* [19]. The neural connectivity between these brain regions might explain the correlation between the cerebellum integrity and cognitive inhibition.

Previous studies investigating the neural correlates of cognitive inhibition using the HSCT have mostly highlighted the contribution of prefrontal regions[5-11]. Even though the cerebellum has traditionally been considered to be mainly involved in motor abilities, many studies have highlighted its role in cognitive inhibition. In the present study, we found significant associations between the HSCT time to completion (part B – part A) and GM in posterior cerebellar regions (such as the vermis VIIb, vermis crusII, and lobules IX, VI and VIIIb). In this vein, Kansal and colleagues have proposed a detailed mapping of the cerebellum in a large cohort of patients with mixed subtypes of cerebellar neurodegenerative disease, [41] and they showed associations between the posterior lobe of the cerebellum and cognitive tasks (versus associations between the anterior lobe of the cerebellum and motor tasks) [41]. In turn, Reetz and colleagues have shown that the posterior lobe of the cerebellum shows stronger functional connectivity with fronto-temporo-parietal areas, the insula and the thalamus (regions implicated in cognitive and affective processes) [42]. These previous studies are in line with our results. More generally, brain-behavior relationships between these specific posterior cerebellar regions and cognitive inhibition or executive tasks implying cognitive inhibition have also been reported: Stroop test and GM volume in the vermis crusII [43], Go/no-go task and GM volume in the vermis lobule VI [44] and finally, Wisconsin Card Sorting task and GM volume in the vermis VIIb [43]. Finally,

a recent study has also shown that transcranial direct current stimulation over the medial cerebellum reduced the percentage of errors during a Go/no-go task [45].

Interestingly, cerebellar atrophy has also been associated with other symptoms in C9+ individuals, more precisely with anxiety [46], psychosis [47] and deranged body schema processing [48]. In this vein, a study recently conducted on patients affected by Friedreich ataxia, a neurodegenerative pathology targeting the dentate nucleus of cerebellum (especially the myelinated efferent white matter fibers), have shown that only the performances on the HSCT were impaired, but not those on other tests assessing the cognitive inhibition (as the Stroop and the Trial Making Test) [49]. Conversely, a recent study in symptomatic C9+ individuals affected by ALS and also showing cerebellar atrophy did not show any correlation with cognitive symptoms, including cognitive inhibition [50]. This result is most probably due to the different neuropsychological measure specifically used in this study (namely the Stroop), and the patients' clinical phenotype (ALS).

To conclude, the HSCT is a useful tool to detect early cognitive changes in C9+ and to predict the progression from the pre-symptomatic to the symptomatic phase. Moreover, the observed relationship between impaired performance and cerebellar damage could reflect a disturbance of cortico-thalamo-cerebellar connectivity. More precisely, C9+ individuals might have impaired access to frontal areas critical for successful cognitive inhibition. Future studies should investigate cognitive inhibition using the HSCT on the full spectrum, ranging from pre-symptomatic subjects to symptomatic patients and possibly using a control group including individuals that do not come from families affected with dementia. Furthermore, future longitudinal studies should directly investigate the potential of the HSCT as a marker of disease progression for the

development of new disease-modifying treatments against FTD and ALS. Also, the association between cognitive inhibition impairments and the connectivity between the cerebellum and other key regions in FTD-ALS associated to *C9orf72* expansion should be explored.

Acknowledgements

Members of the PREV-DEMALS study group: Carole Aubier Girard (CHU Rouen), Eve Benchetrit (Hôpital Pitié-Salpêtrière, Paris), Hugo Bertin (Hôpital de la Salpêtrière, Paris), Anne Bertrand (Hôpital Pitié-Salpêtrière, Paris), Sandrine Bioux (CHU Rouen), Anne Bissery (Hôpital Pitié-Salpêtrière, Paris), Évangéline Bliaux (CHU Rouen), Stéphanie Bombois (CHU Roger Salengro, Lille), Marie-Paule Boncoeur (CHU Limoges), Pascaline Cassagnaud (CHU Roger Salengro, Lille), Mathieu Chastan (CHU Charles Nicolle, Rouen), Yaohua Chen (CHU Roger Salengro, Lille), Marie Chupin (CATI, ICM, Paris), Olivier Colliot (ICM, Paris), Philippe Couratier (CHU Limoges), Xavier Delbeuck (CHU Roger Salengro, Lille), Vincent Deramecourt (CHU Roger Salengro, Lille), Christine Delmaire (CHU Roger Salengro, Lille), Emmanuel Gerardin (CHU Charles Nicolle, Rouen), Claude Hossein-Foucher (CHU Roger Salengro, Lille), Bruno Dubois (Hôpital Pitié- Salpêtrière, Paris), Marie-Odile Habert (Hôpital Pitié-Salpêtrière, Paris), Didier Hannequin (CHU Charles Nicolle, Rouen), Géraldine Lautrette (CHU Limoges), Thibaud Lebouvier (CHU Roger Salengro, Lille), Isabelle Le Ber (Hôpital Pitié-Salpêtrière Salpêtrière, Paris), Stéphane Lehéricy (Hôpital Pitié-Salpêtrière Salpêtrière, Paris), Benjamin Le Toullec (ICM, Paris), Richard Levy (Hôpital Pitié-Salpêtrière Salpêtrière, Paris), Olivier Martinaud (CHU Charles Nicolle, Rouen), Kelly Martineau (CATI, ICM, Paris), Marie-Anne Mackowiak (CHU Roger Salengro, Lille), Jacques Monteil (CHU Limoges), Florence Pasquier (CHU Roger Salengro, Lille), Grégory Petyt (CHU Roger Salengro, Lille), Pierre-François Pradat (Hôpital Pitié-Salpêtrière, Paris), Dorothée Pouliquen (CHU Rouen), Assi-Hervé Oya (Hôpital Pitié-Salpêtrière, Paris), Daisy Rinaldi (Hôpital Pitié-Salpêtrière, Paris), Adeline Rollin-Sillaire (CHU Roger Salengro, Lille),

François Salachas (Hôpital Pitié-Salpêtrière, Paris), Sabrina Sayah (Hôpital Pitié-Salpêtrière, Paris), David Wallon (CHU Rouen).

Funding

This study was funded by grant ANR/DGOS PRTS 2015-2019 PREV-DEMALS from the Assistance Publique–Hôpitaux de Paris (Dr Le Ber) and by grant ANR-10-IAIHU-06 from the Agence Nationale de la Recherche. The study was conducted with the support of the Centre d'Investigation Clinique and the Centre pour l'Acquisition et le Traitement des Images platform.

Maxime Montembeault is supported by Canadian Institute of Health Research (CIHR) and Fonds de recherche du Québec en Santé (FRQS) postdoctoral fellowships.

Competing interests

There are no conflicts of interest for any of the authors.

Figures

Figure 1. Performance on the HSCT in C9- and C9+ individuals according to age.

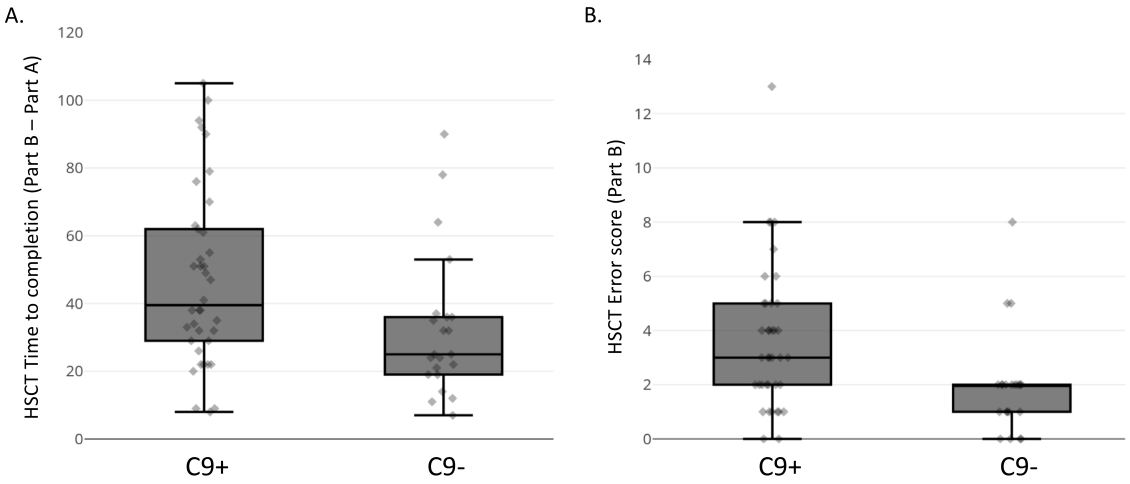

Figure 2. Cerebellar regions in which gray matter volume correlates with HSCT time to completion (part B – part A); $p \leq .05$ FWE cluster level corrected in A) the complete sample and B) C9+ individuals.

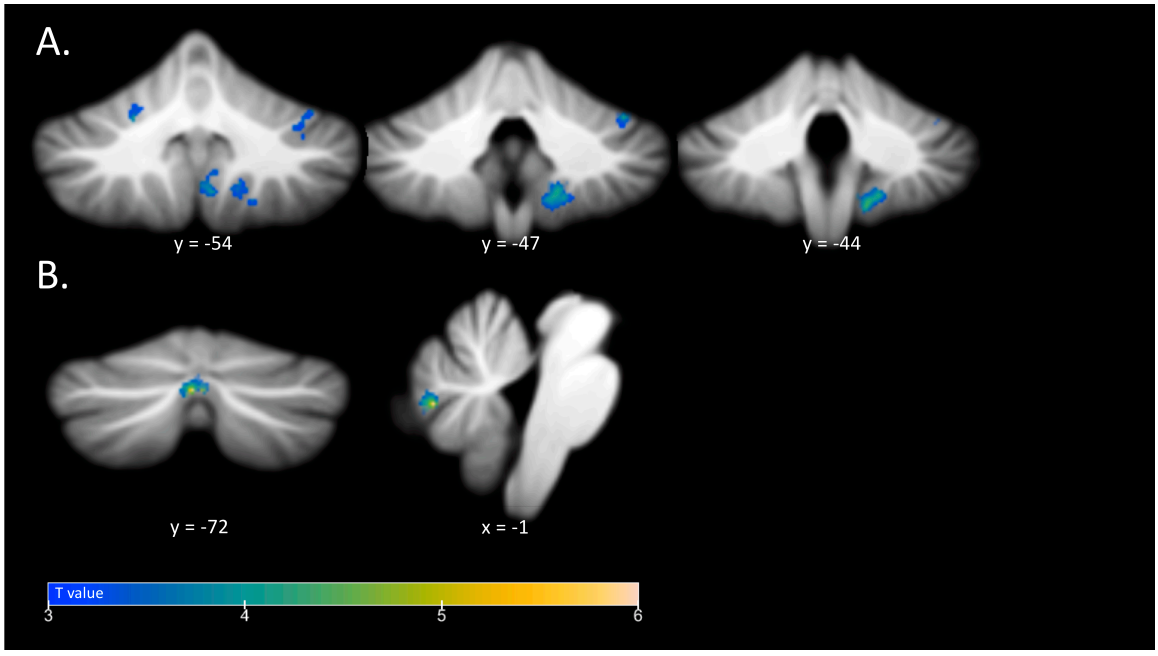

References

1. Odhuba RA, van den Broek MD, Johns LC. Ecological validity of measures of executive functioning. *Br J Clin Psychol* 2005;44(Pt 2):269-78. doi: 10.1348/014466505x29431 [published Online First: 2005/07/12]
2. Burgess PW, Alderman N, Forbes C, et al. The case for the development and use of "ecologically valid" measures of executive function in experimental and clinical neuropsychology. *J Int Neuropsychol Soc* 2006;12(2):194-209. doi: 10.1017/s1355617706060310 [published Online First: 2006/04/01]
3. Haldane M, Cunningham G, Androutsos C, et al. Structural brain correlates of response inhibition in Bipolar Disorder I. *Journal of psychopharmacology (Oxford, England)* 2008;22(2):138-43. doi: 10.1177/0269881107082955 [published Online First: 2008/03/01]
4. Martyr A, Boycheva E, Kudlicka A. Assessing inhibitory control in early-stage Alzheimer's and Parkinson's disease using the Hayling Sentence Completion Test. *Journal of neuropsychology* 2017 doi: 10.1111/jnp.12129 [published Online First: 2017/06/22]
5. Cipolotti L, Spano B, Healy C, et al. Inhibition processes are dissociable and lateralized in human prefrontal cortex. *Neuropsychologia* 2016;93(Pt A):1-12. doi: 10.1016/j.neuropsychologia.2016.09.018 [published Online First: 2016/10/30]
6. Robinson GA, Cipolotti L, Walker DG, et al. Verbal suppression and strategy use: a role for the right lateral prefrontal cortex? *Brain* 2015;138(Pt 4):1084-96. doi: 10.1093/brain/awv003 [published Online First: 2015/02/11]
7. Volle E, de Lacy Costello A, Coates LM, et al. Dissociation between verbal response initiation and suppression after prefrontal lesions. *Cereb Cortex* 2012;22(10):2428-40. doi: 10.1093/cercor/bhr322 [published Online First: 2011/11/19]
8. Hornberger M, Geng J, Hodges JR. Convergent grey and white matter evidence of orbitofrontal cortex changes related to disinhibition in behavioural variant frontotemporal dementia. *Brain* 2011;134(Pt 9):2502-12. doi: 10.1093/brain/awr173 [published Online First: 2011/07/26]
9. Matias-Guiu JA, Cabrera-Martin MN, Valles-Salgado M, et al. Inhibition impairment in frontotemporal dementia, amyotrophic lateral sclerosis, and Alzheimer's disease: clinical assessment and metabolic correlates. *Brain Imaging Behav* 2019;13(3):651-59. doi: 10.1007/s11682-018-9891-3 [published Online First: 2018/05/12]
10. O'Callaghan C, Naismith SL, Hodges JR, et al. Fronto-striatal atrophy correlates of inhibitory dysfunction in Parkinson's disease versus behavioural variant frontotemporal dementia. *Cortex* 2013;49(7):1833-43. doi: 10.1016/j.cortex.2012.12.003 [published Online First: 2013/01/12]
11. Santillo AF, Lundblad K, Nilsson M, et al. Grey and White Matter Clinico-Anatomical Correlates of Disinhibition in Neurodegenerative Disease. *PloS one* 2016;11(10):e0164122. doi: 10.1371/journal.pone.0164122
12. Hornberger M, Savage S, Hsieh S, et al. Orbitofrontal dysfunction discriminates behavioral variant frontotemporal dementia from Alzheimer's disease. *Dement Geriatr Cogn Disord* 2010;30(6):547-52. doi: 10.1159/000321670 [published Online First: 2011/01/22]

13. DeJesus-Hernandez M, Mackenzie IR, Boeve BF, et al. Expanded GGGGCC hexanucleotide repeat in noncoding region of C9ORF72 causes chromosome 9p-linked FTD and ALS. *Neuron* 2011;72(2):245-56. doi: 10.1016/j.neuron.2011.09.011 [published Online First: 2011/09/29]
14. Renton AE, Majounie E, Waite A, et al. A hexanucleotide repeat expansion in C9ORF72 is the cause of chromosome 9p21-linked ALS-FTD. *Neuron* 2011;72(2):257-68. doi: 10.1016/j.neuron.2011.09.010 [published Online First: 2011/09/29]
15. Panman JL, Jiskoot LC, Bouts MJRJ, et al. Gray and white matter changes in presymptomatic genetic frontotemporal dementia: a longitudinal MRI study. *Neurobiol Aging* 2019;76:115-24. doi: https://doi.org/10.1016/j.neurobiolaging.2018.12.017
16. Popuri K, Dowds E, Beg MF, et al. Gray matter changes in asymptomatic C9orf72 and GRN mutation carriers. *NeuroImage Clinical* 2018;18:591-98. doi: 10.1016/j.nicl.2018.02.017 [published Online First: 2018/05/31]
17. Walhout R, Schmidt R, Westeneng HJ, et al. Brain morphologic changes in asymptomatic C9orf72 repeat expansion carriers. *Neurology* 2015;85(20):1780-8. doi: 10.1212/wnl.0000000000002135 [published Online First: 2015/10/27]
18. Bertrand A, Wen J, Rinaldi D, et al. Early Cognitive, Structural, and Microstructural Changes in Presymptomatic C9orf72 Carriers Younger Than 40 Years. *JAMA neurology* 2018;75(2):236-45. doi: 10.1001/jamaneurol.2017.4266 [published Online First: 2017/12/03]
19. Lee SE, Sias AC, Mandelli ML, et al. Network degeneration and dysfunction in presymptomatic C9ORF72 expansion carriers. *NeuroImage Clinical* 2017;14:286-97. doi: 10.1016/j.nicl.2016.12.006 [published Online First: 2016/01/01]
20. Papma JM, Jiskoot LC, Panman JL, et al. Cognition and gray and white matter characteristics of presymptomatic C9orf72 repeat expansion. *Neurology* 2017;89(12):1256-64. doi: 10.1212/wnl.0000000000004393 [published Online First: 2017/09/01]
21. Rohrer JD, Nicholas JM, Cash DM, et al. Presymptomatic cognitive and neuroanatomical changes in genetic frontotemporal dementia in the Genetic Frontotemporal dementia Initiative (GENFI) study: a cross-sectional analysis. *The Lancet Neurology* 2015;14(3):253-62. doi: 10.1016/s1474-4422(14)70324-2 [published Online First: 2015/02/11]
22. Cash DM, Bocchetta M, Thomas DL, et al. Patterns of gray matter atrophy in genetic frontotemporal dementia: results from the GENFI study. *Neurobiol Aging* 2018;62:191-96. doi: 10.1016/j.neurobiolaging.2017.10.008 [published Online First: 2017/11/25]
23. Agosta F, Ferraro PM, Riva N, et al. Structural and functional brain signatures of C9orf72 in motor neuron disease. *Neurobiol Aging* 2017;57:206-19. doi: 10.1016/j.neurobiolaging.2017.05.024 [published Online First: 2017/07/02]
24. Burgess PW, Shallice T. Response suppression, initiation and strategy use following frontal lobe lesions. *Neuropsychologia* 1996;34(4):263-72.
25. Belleville S, Rouleau N, Van der Linden M. Use of the Hayling task to measure inhibition of prepotent responses in normal aging and Alzheimer's disease. *Brain Cogn* 2006;62(2):113-19. doi: https://doi.org/10.1016/j.bandc.2006.04.006

26. Ashburner J. A fast diffeomorphic image registration algorithm. *Neuroimage* 2007;38(1):95-113. doi: http://dx.doi.org/10.1016/j.neuroimage.2007.07.007
27. Ashburner J, Friston KJ. Voxel-Based Morphometry—The Methods. *Neuroimage* 2000;11(6):805-21. doi: http://dx.doi.org/10.1006/nimg.2000.0582
28. Diedrichsen J. A spatially unbiased atlas template of the human cerebellum. *Neuroimage* 2006;33(1):127-38. doi: 10.1016/j.neuroimage.2006.05.056 [published Online First: 2006/08/15]
29. Diedrichsen J, Balsters JH, Flavell J, et al. A probabilistic MR atlas of the human cerebellum. *Neuroimage* 2009;46(1):39-46. doi: 10.1016/j.neuroimage.2009.01.045 [published Online First: 2009/05/22]
30. Diedrichsen J, Maderwald S, Kuper M, et al. Imaging the deep cerebellar nuclei: a probabilistic atlas and normalization procedure. *Neuroimage* 2011;54(3):1786-94. doi: 10.1016/j.neuroimage.2010.10.035 [published Online First: 2010/10/23]
31. Diedrichsen J, Zotow E. Surface-Based Display of Volume-Averaged Cerebellar Imaging Data. *PloS one* 2015;10(7):e0133402. doi: 10.1371/journal.pone.0133402 [published Online First: 2015/08/01]
32. Jiskoot LC, Panman JL, van Asseldonk L, et al. Longitudinal cognitive biomarkers predicting symptom onset in presymptomatic frontotemporal dementia. *J Neurol* 2018;265(6):1381-92. doi: 10.1007/s00415-018-8850-7 [published Online First: 2018/04/09]
33. Balendra R, Isaacs AM. C9orf72-mediated ALS and FTD: multiple pathways to disease. *Nature reviews Neurology* 2018;14(9):544-58. doi: 10.1038/s41582-018-0047-2 [published Online First: 2018/08/19]
34. Lee YB, Baskaran P, Gomez-Deza J, et al. C9orf72 poly GA RAN-translated protein plays a key role in amyotrophic lateral sclerosis via aggregation and toxicity. *Hum Mol Genet* 2017;26(24):4765-77. doi: 10.1093/hmg/ddx350 [published Online First: 2017/10/04]
35. Irwin DJ, McMillan CT, Brettschneider J, et al. Cognitive decline and reduced survival in C9orf72 expansion frontotemporal degeneration and amyotrophic lateral sclerosis. *Journal of Neurology, Neurosurgery & Psychiatry* 2013;84(2):163-69. doi: 10.1136/jnnp-2012-303507
36. Whitwell JL, Boeve BF, Weigand SD, et al. Brain atrophy over time in genetic and sporadic frontotemporal dementia: a study of 198 serial magnetic resonance images. *Eur J Neurol* 2015;22(5):745-52. doi: 10.1111/ene.12675 [published Online First: 2015/02/17]
37. Whitwell JL, Weigand SD, Boeve BF, et al. Neuroimaging signatures of frontotemporal dementia genetics: C9ORF72, tau, progranulin and sporadics. *Brain* 2012;135(Pt 3):794-806. doi: 10.1093/brain/aws001 [published Online First: 2012/03/01]
38. Mahoney CJ, Beck J, Rohrer JD, et al. Frontotemporal dementia with the C9ORF72 hexanucleotide repeat expansion: clinical, neuroanatomical and neuropathological features. *Brain* 2012;135(3):736-50. doi: 10.1093/brain/awr361
39. Bocchetta M, Cardoso MJ, Cash DM, et al. Patterns of regional cerebellar atrophy in genetic frontotemporal dementia. *NeuroImage: Clinical* 2016;11:287-90. doi: https://doi.org/10.1016/j.nicl.2016.02.008
40. Behrens TE, Johansen-Berg H, Woolrich MW, et al. Non-invasive mapping of connections between human thalamus and cortex using diffusion imaging. *Nat*

Neurosci 2003;6(7):750-7. doi: 10.1038/nn1075 [published Online First: 2003/06/17]
41. Kansal K, Yang Z, Fishman AM, et al. Structural cerebellar correlates of cognitive and motor dysfunctions in cerebellar degeneration. *Brain* 2017;140(3):707-20. doi: 10.1093/brain/aww327 [published Online First: 2017/01/04]
42. Reetz K, Dogan I, Rolfs A, et al. Investigating function and connectivity of morphometric findings--exemplified on cerebellar atrophy in spinocerebellar ataxia 17 (SCA17). *Neuroimage* 2012;62(3):1354-66. doi: 10.1016/j.neuroimage.2012.05.058 [published Online First: 2012/06/05]
43. Olivito G, Lupo M, Iacobacci C, et al. Structural cerebellar correlates of cognitive functions in spinocerebellar ataxia type 2. *J Neurol* 2018;265(3):597-606. doi: 10.1007/s00415-018-8738-6 [published Online First: 2018/01/23]
44. Lupo M, Olivito G, Iacobacci C, et al. The cerebellar topography of attention sub-components in spinocerebellar ataxia type 2. *Cortex* 2018;108:35-49. doi: 10.1016/j.cortex.2018.07.011 [published Online First: 2018/08/20]
45. Wynn SC, Driessen JMA, Glennon JC, et al. Cerebellar Transcranial Direct Current Stimulation Improves Reactive Response Inhibition in Healthy Volunteers. *Cerebellum (London, England)* 2019;18(6):983-88. doi: 10.1007/s12311-019-01047-z [published Online First: 2019/06/10]
46. Sellami L, Bocchetta M, Masellis M, et al. Distinct Neuroanatomical Correlates of Neuropsychiatric Symptoms in the Three Main Forms of Genetic Frontotemporal Dementia in the GENFI Cohort. *Journal of Alzheimer's disease : JAD* 2018;65(1):147-63. doi: 10.3233/jad-180053 [published Online First: 2018/07/17]
47. Devenney EM, Landin-Romero R, Irish M, et al. The neural correlates and clinical characteristics of psychosis in the frontotemporal dementia continuum and the C9orf72 expansion. *NeuroImage Clinical* 2016;13:439-45. doi: 10.1016/j.nicl.2016.11.028
48. Downey LE, Fletcher PD, Golden HL, et al. Altered body schema processing in frontotemporal dementia with C9ORF72 mutations. *Journal of Neurology, Neurosurgery & Psychiatry* 2014;85(9):1016-23. doi: 10.1136/jnnp-2013-306995
49. Corben LA, Klopper F, Stagnitti M, et al. Measuring Inhibition and Cognitive Flexibility in Friedreich Ataxia. *Cerebellum (London, England)* 2017;16(4):757-63. doi: 10.1007/s12311-017-0848-7 [published Online First: 2017/02/24]
50. Consonni M, Dalla Bella E, Nigri A, et al. Cognitive Syndromes and C9orf72 Mutation Are Not Related to Cerebellar Degeneration in Amyotrophic Lateral Sclerosis. *Frontiers in Neuroscience* 2019;13(440) doi: 10.3389/fnins.2019.00440